Supporting information

Dynamic switching of helical microgel ribbons

Hang Zhang[#], Ahmed Mourran[#]*, Martin Möller[#+]*,

[#]DWI - Leibniz-Institute for Interactive Materials,
[+]Institute of Technical and Macromolecular Chemistry der RWTH Aachen University
Forckenbeckstr. 50, D-52056, Aachen (Germany)

*To whom correspondence should be sent, E-mail: mourran@dwi.rwth-aachen.de; moeller@dwi.rwth-aachen.de

List of content

1. Synthesis of gold nanorods (AuNRs)

Gold nanorods (AuNRs) were synthesized by a seed-mediated method.[1] All chemicals were purchased from Sigma-Aldrich if not otherwise mentioned. Deionized water (0.1 µS/cm, ELGA Purelab-Plus) was used. For the seed solution, 0.60 mL of freshly prepared ice-cold 0.010 M $NaBH_4$ (99%) aqueous solution was added to a mixture of water (4.2 mL), 0.20 M Cetyltrimethylammonium bromide (CTAB, 5.0 mL, 99%) and 0.0030 M hydrogen tetrachloroauric (III) acid ($HAuCl_4$, 0.83 mL, p.a.) under vigorous stirring for 2 min. For the growth solution, 0.20 M CTAB (150 mL), 0.050 M ascorbic acid (3.1 mL, 99%) and 0.0080 M $AgNO_3$ (3.3 mL, 99.99%) were added under stirring to 0.0010 M $HAuCl_4$ (150 mL). The temperature of the growth solution was kept at 25 °C in water bath, and 0.875 mL of seed solution were injected under rigorous stirring followed by 30 min of stirring and addition of 0.050 M ascorbic acid (2.0 mL) at a flow rate of 0.50 mL/h. Afterwards the solution was stirred for another 30 min. The resultant brownish red solution of AuNRs was centrifuged at 8000 rpm for 40 min in an Eppendorf Centrifuge 5810. The supernatant containing excess surfactant was discarded, and the precipitated AuNRs were collected and re-suspended in water with a final volume of ca. 20 mL.

Surface modification of AuNRs: Thiol functional polyethylene glycol (PEG) polymer (HS-PEG-OH, Mw = 3000 Da, Iris Biotech) was dissolved in ethanol (99.8%) to make a 2.5 mM solution. 10 mL of the solution with redispersed AuNRs were diluted to 100 mL and mixed with 20 mL ethanolic PEG solution under stirring. This solution was sonicated at 60 °C for 30 min and subsequently for another 3.5 h at 30 – 50 °C.[2] After stirring of the solution overnight, it was extracted three times with chloroform (ca. 120 mL, p.a.) to remove CTAB and free polymer. In a second purification step, the extracted solution was centrifuged for 3 times, each time the supernatant was discarded and the sedimented gold-containing fraction (less than 2 mL) was diluted with dimethyl sulfoxide (DMSO) to 45 mL. After the last centrifugation, the sedimented gold-containing fraction was collected as a concentrated solution of PEGylated AuNRs in DMSO. The modified AuNRs had a longitudinal absorption band maximum at 791 nm (UV-Vis spectrum, V-630, JASCO). Transmission electron microscopy (Libra 120, Zeiss) revealed that the AuNRs had an average diameter of 15.4 nm and length of 60.0 nm, i.e. an aspect ratio of 3.90, see **Figure S1**.

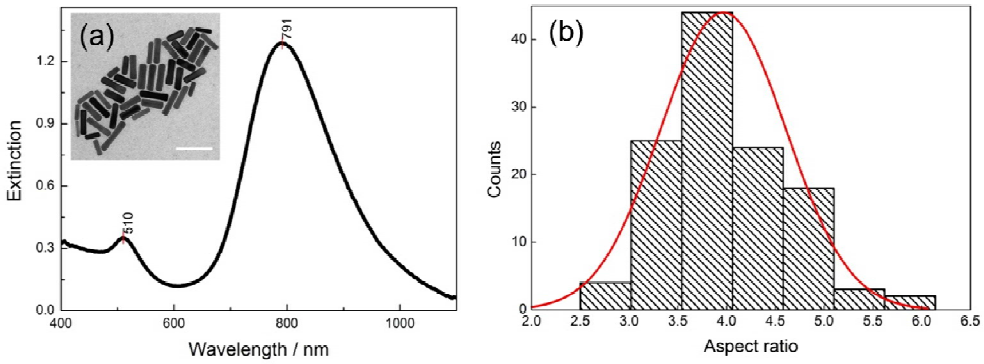

Figure S1. (a) UV-Vis spectrum of PEGylated AuNRs with inset of TEM micrograph (500 × dilution in water, optical path = 1 cm, scale bar: 100 nm). Optical density (OD) at 791nm = 1.288, OD at 808 nm = 1.258. (b) Statistics of PEGylated AuNR, 120 particles were analyzed with ImageJ. Red curve is the Gaussian fitting.

2. Gold nanorods loaded microgels

Table S1 summarizes the composition of the solution for the preparation of microgels. Crosslinker (N,N'-Methylenebisacrylamide, BIS, 99%) and photo-initiator (2-Hydroxy-4′-(2-hydroxyethoxy)-2-methylpropiophenone, 98%) were added at a molar amount of 1 % relative to N-Isopropylacrylamide (NIPAm, 97%, recrystallized twice in n-hexane). After addition of an appropriate volume of the gold nanorod solution, the light extinction maximum is at 791 nm (longitudinal plasmonic band of the AuNRs). For an optical path length of 1 cm, it resulted in an optical density of 240.

Table S1. Composition of monomer solution

	NIPAm	BIS	Photo-initiator	AuNR	DMSO
Microparticles	57.5 mg	0.783 mg	1.14 mg	57.5 µL	40.6 µL

The number density of AuNRs in the monomer solution was calculated according to Equation 1 to 3, where T is the transmission, σ is the extinction cross-section of AuNRs, n is the number density of AuNRs, l is the optical path, and OD is the optical density.

$$T = e^{-\sigma n l} \qquad (1)$$

$$OD = -\log T \qquad (2)$$

$$n = 2.3(OD/\sigma l) \qquad (3)$$

By assuming σ to be ~ 6100 nm^2 at wavelength of 791 nm for the AuNRs used in the present study,[3] the number density can be calculated to be 3.8 μm^{-3} for *OD* = 100 solution and 9.1 μm^{-3} for the *OD* = 240 solution.

Preparation of perfluoropolyether replica: The microgel ribbon was fabricated in a non-wetting template made of perfluoropolyether (PFPE), which is the negative replica of a photo-lithographically patterned silicon wafer.[4] In a glove box, a cleaned microscope slide was placed on top of a diced silicon master (2 cm × 2 cm) produced by photolithography (AMO GmbH), while two pieces of bilayer parafilm (Bemis, total thickness ~ 200 µm) were used as spacers. Details of silicon masters with 5 µm etching depth can be found in **Figure S2**. Other silicon masters are of the same structural design but different etching depths. Perfluoropolyether-urethane dimethacrylate (PFPE, M_w = 2000, Fluorolink MD700, Solvay Solexis) was thoroughly mixed with 1 wt% Darocure 1173 (Ciba Specialty Chemicals), which is the photoinitiator. The mixture was then injected between the glass slide and silicon master until the space was fully filled. Subsequently, the PFPE was cured for 20 min under a UV lamp (366 & 254nm, 2 × 4 W, Konrad Benda) in an Argon atmosphere. After curing, the PFPE film was carefully peeled off from silicon master and cut into suitable size (6 mm × 6 mm). The flat PFPE film was prepared by the same protocol between two microscope slides.

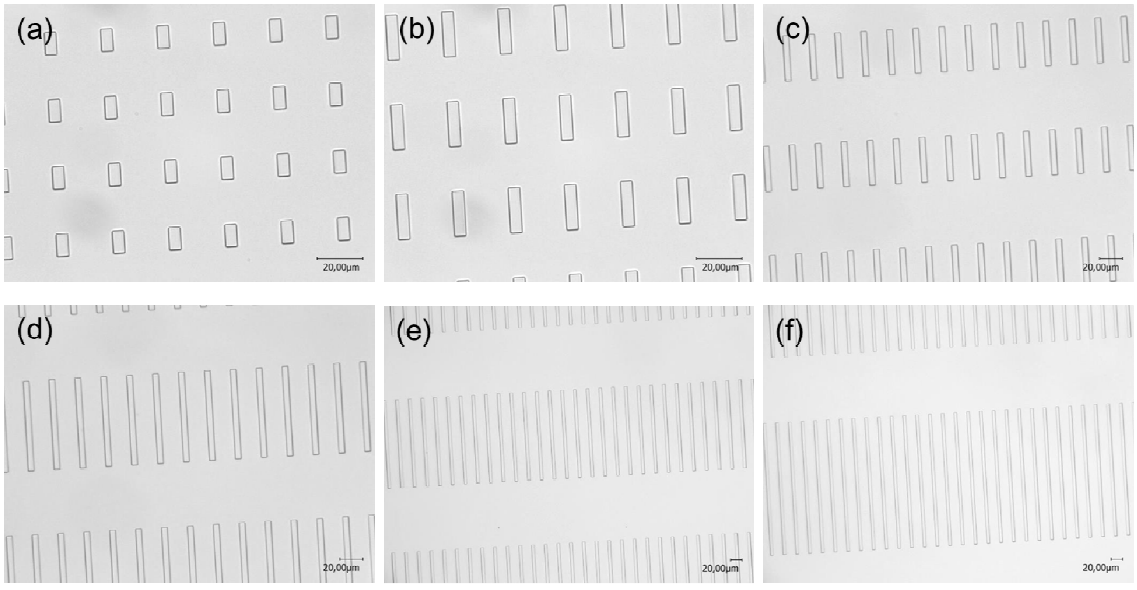

Figure S2. Optical micrographs of the silicon masters with an etching depth of 1 µm. The width is 5 µm for all the ribbons. The lengths from (a) to (f) are 10 µm, 20 µm, 40 µm, 80 µm, 160 µm, and 240 µm, respectively. Scale bar: 20 µm.

Fabrication and harvest of anisometric microgel particles: The fabrication procedure is illustrated in **Figure S3**. A home-made press with quartz window was used for the molding of microgel, and all steps were carried out in a glove box (O_2 < 0.2%). The monomer solution (0.5 µL) was first pipetted on the replicated PFPE film, which was then covered by a flat PFPE film. A weight was applied on top of the flat film to generate suitable pressure (~ 260 kPa) to the mold. The pressure ensures that only separate elements were formed. The microgels were cured by 20 min of UV irradiation (366 & 254nm, 4 W of each wavelength, Konrad Benda). Afterwards the weight was removed, and the mold was peeled off from the flat film. Bi-layered microgels were produced by sputtering a thin gold film (~ 2 nm) on the sample with a sputter coater (30 mA, 20s, Edwards S150B). The affinity between gold and amide group, as well as physical entrapment provides strong adhesion of the metal layer to the gel surface.[5] Indeed, no delamination of the metal layer was observed throughout all our experiments. The prepared microgels have certain stickiness to the mold after curing. Therefore, an extra step to transfer and release the microgel is needed.

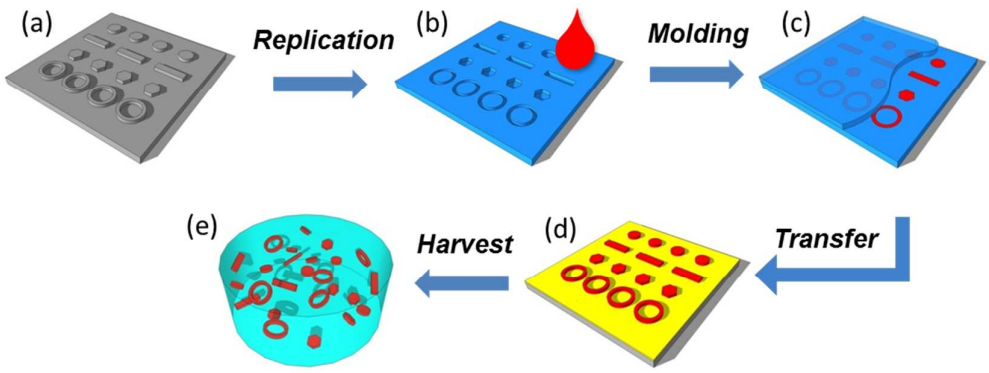

Figure S3. Illustration of the microfabrication process. (a) Micropatterned silicon master; (b) Replicated PFPE mold; (c) Molding of microgel particles; (d) Transfer of microgel particles on adhesive layer (yellow); (e) Released microgel particles in water.

Microscope slides (Corning glass) were cut into squares (25 × 25 mm) and cleaned with sonication in isopropanol. 0.5 mm thick PDMS film (Sylgard 184, Dow Corning) was cut into square frame with outer dimension of 15 mm × 15 mm and inner dimension of 10 × 10 mm. The cleaned glass slide and the PDMS frame were activated in O_2 plasma (200 W, 20 s, 1 mbar, PVP Tepla 100) and then bound together to form an open chamber. Glycerol (15 µL, 99.5%) was pipetted in the chamber and the PFPE mold with hydrogel particles was placed upside down in the chamber. The whole chamber was then stored in a freezer at -80 °C

overnight. Transfer of the microgels was achieved by peeling the PFPE mold off, where the frozen glycerol served as adhesive. The glycerol was subsequently evaporated at 60°C under vacuum (1×10^{-2} mbar), leaving only microgels in the PDMS chamber. Deionized water was added to reswell the microgel. To load the microgels into capillary, one end of a plasma-treated rectangular capillary (0.05 × 1.0 × 50 mm, Vitrocom) was immersed in the chamber, so that the microgels can be spontaneously sucked in by capillary force. The ends of the capillary (200 W, 20 s, 1 mbar) were then sealed and fixed on a microscope slide with a 2-component epoxy adhesive (UHU GmbH).

3. **Microscopy observation of helical microgel at different temperatures**

The capillary containing microgels was placed on a home-made Peltier stage for temperature control. The Peltier stage was mounted on an optical microscope stage (VHZ-100UR, Keyence). The temperature of sample was controlled with an accuracy of ± 0.1 °C. Images were taken after the sample was equilibrated for more than 5 min at different temperatures. The images of the microgels were adjusted with ImageJ; the radius and length of the helical microgel were measured manually.

Free swelling of ribbon-shaped microgels*:* The swelling degree of a ribbon-shaped microgel without sputter coating was measured at different temperatures. Three optical micrographs are shown in **Figure S4**. The length of the ribbon was measure with ImageJ and 10 different microgel particles were measured at each temperature to asses the swelling curve in Figure 2C. The linear swelling degree is acquired by normalizing the length of the ribbon at different temperatures to the length of the mold, i.e. 80 μm. The optical contrast is relatively low, since the refractive indices of hydrogel and water are close.

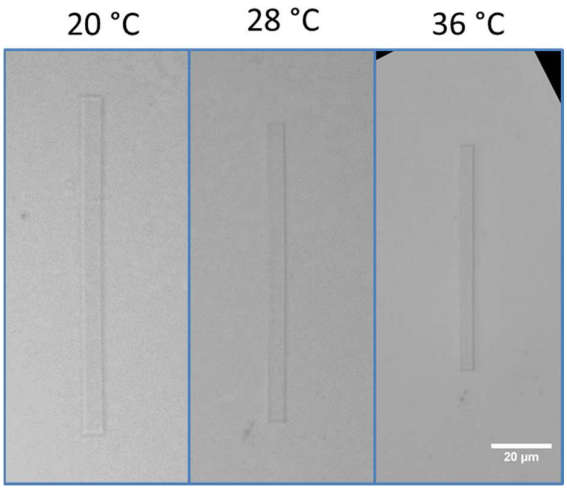

Figure S4. Ribbon-shaped microgel without coating at different temperatures. Scale bar: 20 µm

4. Photothermal heating and optical microscopy monitoring of the actuation

The helical microgel was irradiated with a near infrared (NIR) laser (808 nm, 2.5 W, Roithner Lasertechnik) which was focused to the middle of field of view with an incident angle of ~ 40 °. This results in an elliptical footprint (~ 1 mm × 1.5 mm) with an illumination intensity of 1.7 W/mm^2 as measured by an optical power meter (PM200, Thorlab). The laser was modulated with 1 ms temporal resolution. Videos were recorded with a high speed camera (Miro M310, Phantom) at 1000 or 2000 frames per second. A short pass filter (700 nm, OD 4, Edmund optics) was used to protect the camera from scattered laser. Acquired videos were contrast-enhanced and analyzed with ImageJ. Corresponding video can be found in **Video S1**.

Video S1 shows the slow motion video of the helical microgel during one cycle of modulation (80 ms on-time, 12 ms off-time). The laser was switched on at t = 0 ms and switched off at t = 80 ms.

Estimation of equilibration time: The characteristic equilibration time of temperature change inside a microgel particle depends strongly on the size of the particle with a power law $\tau = l^2/D$, since it is essentially a thermal diffusion process. Utilizing the thermal diffusivity of water at 25°C, i.e. $D_{thermal}$ = 0.14 mm^2/s, the characteristic time of thermal equilibration can be approximated for the rectangular capillary (thickness ~ 50 µm) to be roughly 0.18 s and for the microgel ribbon (H ~ 1 µm) to be around 7 µs. This can be compared with the diffusion process of gel network that results in volume change, which has a diffusion coefficient D_p ~ 2

$\times 10^{-11}$ m^2/s at $\Delta T = 3\ °C$ (ΔT is the difference between set temperature and LCST) [6] and is thus orders of magnitude slower than the thermal equilibration. For instance, it can be estimated that 25 milliseconds are needed for the gel to shrink by 0.5 µm under the abovementioned condition. It can also be concluded that the thermal equilibration is always much faster than the volume change inside the microgel due to the huge difference between the two types of diffusivity, so that the temperature change can be considered as an instantaneous process when dealing with the volume change of the gel. Besides, the response dynamics can be strongly enhanced by reducing the dimension of the hydrogel, owning to the fact that the characteristic time of swelling depends on the square of the characteristic length of the microgel.[7]

***Temperature estimation*:** Upon laser irradiation, the temperature of the microgel is increased, so that it undergoes inversion of helicity. At steady state upon irradiation, the inverse helix has a pitch of 11.4 µm which corresponds approximately to the data point at 34 °C (pitch: 11.3 µm) in **Figure S5**. This indicates that the temperature reached is roughly 34 °C by the laser irradiation.

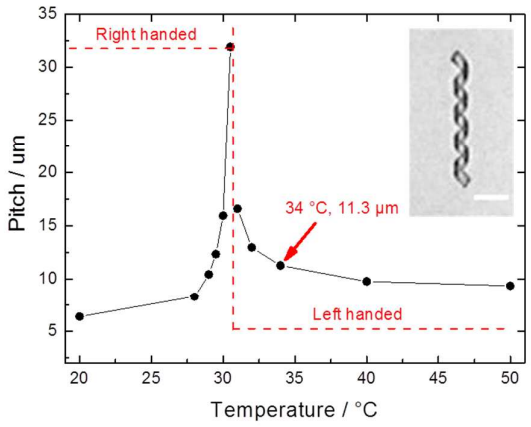

Figure S5. Change of pitch versus temperature at equilibrium. Inset: helix at equilibrated state upon laser irradiation. Scale bar: 15 µm.

5. Effects of salt and temperature on the deformation kinematics

The helical microgels were loaded into a capillary (length = 2 cm, width = 0.1cm height = 50 µm,) and the ends of the capillary were kept open to allows investigating of the same helix exchange at different salt concentration while. The capillary was then placed on a microscope slide for observation. To avoid water evaporation, the videos were immediately captured by a high-speed camera at a frame rate of 2000 fps. Subsequently, the capillary was immersed in

reservoir of Na_2SO_4 solutions (99.0%, 0.01M and 0.02M). After equilibration of the ions inside the capillary (> 48 hours), the same helix was used again for video record at the same modulation. The videos of the helix under 120 ms – 30 ms stroboscopic irradiation can be found in supporting videos. This modulation was chosen as it provides inversion of the chirality at different salt concentrations. The comparison of water with 0.02 M can be found in Video S3.

For the temperature-dependent experiments, the capillary containing microgel was sealed by epoxy glue and fixed on a microscope slide. The bath temperature was controlled by the peltier stage beneath the slide with an accuracy of ± 0.1 °C. Videos were recorded by the high-speed camera with a frame rate of 2000 fps. The stroboscopic irradiation was 120 ms (on) – 30 ms (off). The time for the helix to reach the fully stretched shape (t_1) was measured using ImageJ. The error bar in Figure 5 is due to the temporal resolution of the video and the inaccuracy in determining the frame of helical inversion. The comparison of 20 °C with 21.5 °C can be found in Video S2.

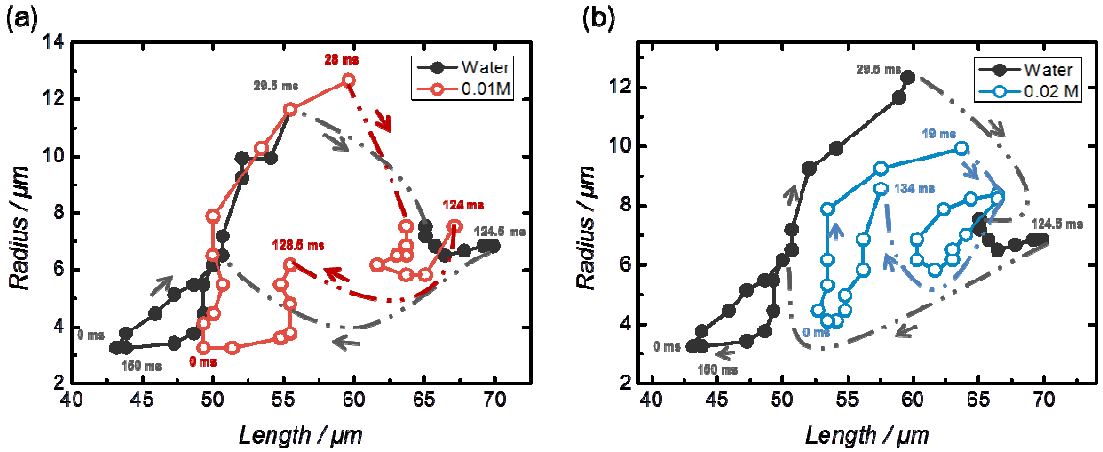

Figure S6. Change of radius versus length at different salt concentrations. (a) Helix in water and in 0.01 M Na_2SO_4 solution. (b) Helix in water and in 0.02 M Na_2SO_4 solution. Stroboscopic irradiation period: 120 ms (on) – 30 ms (off). The arrow marks the direction of change, and the dotted lines in the reversal process are to guide the eyes.

Figure S6 shows the kinematics of the helix under stroboscopic irradiations for different salt concentrations, which was quantitatively measured by ImageJ. The deformation path was significantly altered as the salt concentration increases to 0.02 M as shown in Figure S7 (b).

Supporting videos

Video S1. Slow motion video of a microgel helix undergoing handedness inversion under one irradiation period with an **on/off** time of **80 ms /12 ms**. The video frame rate is **20 fps** which correspond to a slowdown factor of **100**.

Video S2. Slow motion video of helical microgel at different bath temperatures undergoing inversion under one irradiation cycle. On the left movies the water temperature was **20 °C**, while on the right one it was **21.5 °C**. The irradiation period was **120 ms/30 ms** (**on/off**). The video frame rate is **50 fps** which correspond to a slowdown factor of **40**.

Video S3. Slow motion video of a helical microgel under one irradiation cycle at different salt concentrations (**0.0 M** on the left and **0.02 M** on the right). The irradiation has an **on/off** period of **120 ms/30 ms**. The video frame rate is **50 fps** which correspond to a slowdown factor of **40**.

References

1. Nikoobakht, B.; El-Sayed, M. A. *Chem Mater* 2003, 15, (10), 1957-1962.
2. Bartneck, M.; Keul, H. A.; Singh, S.; Czaja, K.; Bornemann, J.; Bockstaller, M.; Moeller, M.; Zwadlo-Klarwasser, G.; Groll, J. *Acs Nano* 2010, 4, (6), 3073-3086.
3. Qin, Z. P.; Bischof, J. C. *Chem Soc Rev* 2012, 41, (3), 1191-1217.
4. Rolland, J. P.; Maynor, B. W.; Euliss, L. E.; Exner, A. E.; Denison, G. M.; DeSimone, J. M. *J Am Chem Soc* 2005, 127, (28), 10096-10100.
5. Hu, Z. B.; Chen, Y. Y.; Wang, C. J.; Zheng, Y. D.; Li, Y. *Nature* 1998, 393, (6681), 149-152.
6. Li, Y.; Tanaka, T. *Annu Rev Mater Sci* 1992, 22, 243-277.
7. Shibayama, M.; Tanaka, T. *Adv Polym Sci* 1993, 109, 1-62.